AIAA JOURNAL
Vol. 37, No. 5, May 1999

Hybrid Optimization Strategy Beyond Local Optima in Aerospace Panel Designs

K. Leung Chan,* David Kennedy,† and Fred W. Williams‡
Cardiff University, Cardiff, Wales CF2 3TB, United Kingdom

Convergence to local optima rather than the global optimum is a common shortcoming of directed search (gradient-based) optimization techniques. Successive convergence on better local optima is an efficient way of finding the global optimum and is achieved by the proposed hybrid global optimization strategy, which combines ideas from the improving hit-and-run and the tunneling global optimization methods. The searching technique of improving hit-and-run is adapted to find suitable starting points to converge on other (better) local optima. The suitability of candidate starting points is confirmed by the concept of the tunneling method. The strategy presented has unique features due to the underlying structural theory being exact, in the sense of differential equations being solved for the member (or element) stiffnesses so that they are transcendental functions of the load factor. Hence the buckling eigenproblem for the entire structure is a transcendental one, instead of the linear one associated with the more usual finite element method formulations. Constrained minimum-mass aerospace panel stability design problems are used to demonstrate the efficiency and robustness of the hybrid global optimization strategy.

I. Introduction

FOR many engineering optimization problems, multiple local optima exist within the multidimensional design space. The best local optimum is deemed to be the global optimum. Finding the global optimum rather than a local optimum is vital in constrained structural optimization problems where mass is at a premium, e.g., in aerospace structures.

There are two main categories of optimization methods: directed search and random search. Directed search optimization methods, which include the optimality criteria[1] and feasible directions[2] methods, use the gradients of the objective function and of the constraints to converge efficiently to the solution but suffer from the drawback of potentially being trapped at a converged local optimum. Purely random search methods, including genetic algorithms[3–6] and simulated annealing,[7] search extensively through the design space at random points for better designs and are increasingly being used in global optimization. Their independence of gradients means that they are less prone to converge to local optima but are relatively computationally expensive as very many objective and constraint function evaluations may be required to guarantee convergence.

The higher computational efficiency of directed search methods, compared with that of random search methods, has motivated much research on how to escape from converged local optima and to find better local optima successively and hence the global optimum. Examples include Levy and Gomez's tunneling method,[8] the improving hit-and-run method (IHR) by Zabinsky et al.[9] and Zabinsky,[10] and the successive approximation method by Snyman and Stander.[11] The tunneling method generally requires the use of penalty functions for constrained problems, and IHR suffers slower convergence for such problems.

We propose in this paper to combine some of the ideas of the tunneling and IHR methods into a hybrid global optimization strategy for solving constrained structural optimization problems. The hybrid strategy does not require the use of penalty functions. Its efficiency and robustness are demonstrated by using the authors' software VICONOPT[12] as a test-bed program to solve example aerospace panel design problems in which an objective function $f(\boldsymbol{X})$ is minimized subject to constraints $g_j(\boldsymbol{X})$ and simple bounds on the design variables, i.e.,

minimize

$$f(\boldsymbol{X}), \qquad \boldsymbol{X} = \{x_1, x_2, \ldots, x_n\}^T \tag{1}$$

subject to

$$g_j(\boldsymbol{X}) \le 0, \qquad j = 1, 2, \ldots, m \tag{2}$$

$$x_{\mathrm{l}i} \le x_i \le x_{\mathrm{u}i}, \qquad i = 1, 2, \ldots, n \tag{3}$$

where m is the number of constraints imposed, $x_{\mathrm{l}i}$ and $x_{\mathrm{u}i}$ are, respectively, lower and upper bounds on each design variable x_i, and n is the number of design variables that can be plate widths, thicknesses, and/or ply-angle orientations of the composite material. For the example problems of this paper, the objective function $f(\boldsymbol{X})$ is simply the panel mass, although more complex models of manufacturing costs could equally be used.[13] The constraints $g_j(\boldsymbol{X})$, which include buckling, material strength, and geometric requirements, commonly lead to the existence of multiple local optima.

The strategy has unique features because of the underlying structural theory being exact, in the sense of differential equations being solved for the member (or element) stiffnesses so that they are transcendental functions of the load factor. Hence, the buckling eigenproblem for the entire structure is a transcendental one, instead of the linear one associated with the more usual finite element method formulations and can be solved iteratively using the Wittrick–Williams algorithm.[14]

II. Optimization Methods

A. Tunneling Method

Figure 1 is a schematic plot of the objective function (i.e., mass) against (generalized) changes to the design variables. Points on or above the solid curve satisfy all of the constraints and therefore represent feasible designs, whereas points below the solid curve represent infeasible designs. The basic concept of the tunneling method[8] is to search in the neighborhood region of the converged local optimum A to find another feasible design C_3 that shares its mass f_A. Because the converged local optimum A is at the base of a valley, the newly found feasible design C_3 of the same mass is guaranteed to be in the valley of a different, but not necessarily better, local optimum B. In physical terms the search has tunneled from the converged local optimum A through a hill into the valley of a different local optimum B. The newly found feasible design C_3 is then used as the starting point from which to converge on this local optimum B. For unconstrained problems the feasible design

Received July 7, 1998; revision received Jan. 8, 1999; accepted for publication Jan. 8, 1999.

*Research Associate, School of Engineering.
†Lecturer, School of Engineering, P.O. Box 686. E-mail: kennedyd@cardiff.ac.uk. Member AIAA.
‡Professor, School of Engineering. Member AIAA.

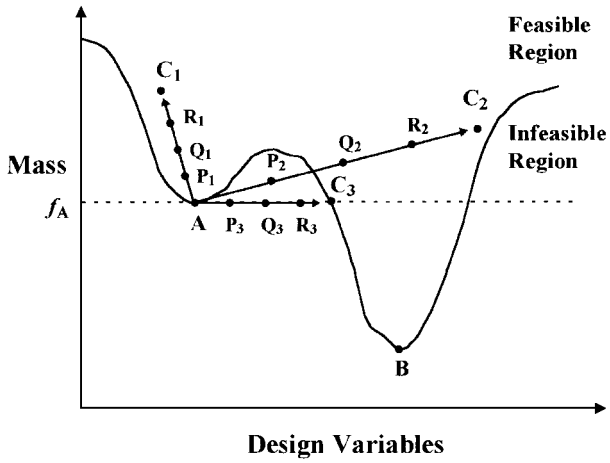

Fig. 1 Possible searching moves to feasible candidate designs C_k (k = 1, 2, and 3). C_1 is within the valley of the previously converged local optimum A of mass f_A. C_2 and C_3 are within the valley of a different, not necessarily better, local optimum B.

C_3 is efficiently found by the use of the tunneling function[8] with a zero-finding algorithm. For constrained problems penalty functions are generally used, and the searching process can be severely hampered as its effectiveness relies on the accuracy of the definitions of the penalty functions. This is why the searching technique of IHR, which does not use penalty functions, has been judged to be more suitable for finding feasible designs for constrained problems in the hybrid global optimization strategy presented in Sec. III.

B. IHR Method

The IHR method[9] is a random search algorithm. At each iteration the method generates a candidate point for improvement, and the iterations are uniformly distributed along a randomly chosen direction within the feasible region. A candidate point is accepted as the next iterate only if it offers improvement over the current best design. The random direction is generated from the multivariate normal distribution with zero mean and covariance matrix $\boldsymbol{H}^{-1}$. IHR achieves the analytically established polynomial convergence performance only when $\boldsymbol{H}$ is positive definite and is set to the Hessian of a quadratic objective function. Slower convergence occurs for other types of problem, such as those considered in this paper, for which the direction distribution is uniform in a hypersphere with $\boldsymbol{H}$ set to the identity matrix. This is why the tunneling method step of converging on the local optimum before proceeding in a randomly chosen direction is preferred in the hybrid global optimization strategy presented in the next section.

III. Hybrid Global Optimization Strategy

The proposed hybrid global optimization strategy first converges on a local optimum using the VICONOPT design procedure, which is based on the method of feasible directions.[2] This local optimum is quite likely to be the one nearest to the (user-specified) initial design and is therefore unlikely to be the global optimum. The proposed strategy next uses the adapted IHR searching technique to find a new valley, which is numerically confirmed to be distinct from the first valley by the tunneling concept. The corresponding local optimum of this newly found valley is then converged on using the VICONOPT design procedure. The global optimum is thus obtained by successively finding and converging on other (better) local optima. The principal steps of this hybrid global optimization strategy are outlined in Fig. 2 and are described in more detail as follows (all step numbers referring to the steps of Fig. 2).

A. Random Directions and Candidate Designs

Each random direction vector is constructed at step 2 from n random numbers lying between zero and one using a uniform random number generator based on the subtractive method.[15] Subtracting these random numbers from a datum value of 0.5 gives the n components of a random direction vector, each lying between -0.5 and 0.5 (so that there is an equal chance of increasing and decreasing each of the design variables from their values at the best local optimum so far converged on). Because the dimensions of the design variables can be of different order, e.g., plate breadths and thicknesses, the positive and negative components of the random direction vector are scaled such that -0.5, 0.5, and 0 represent x_{li}, x_{ui}, and the current value of x_i, respectively. This has the advantage that if any design variable is close to its lower/upper bound at the local optimum, when searching toward the opposite bound, bigger moves away from the local optimum can be made. Thus the search is encouraged to move well away from the local optimum and hence is more likely to escape from it.

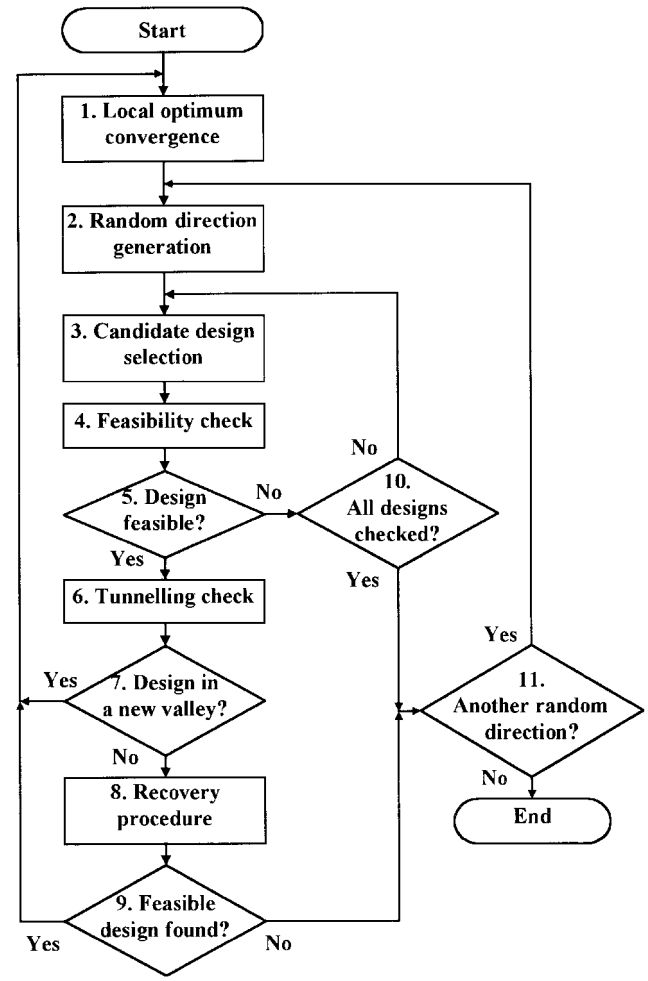

Fig. 2 Steps of the hybrid global optimization strategy.

A number of candidate designs are uniformly distributed along this random direction. This number of candidate designs is determined, for each random direction, in the way described in Sec. IV. Each candidate design is checked in turn for feasibility, starting with the one most remote from the current best local optimum (see steps 3 and 4).

B. Classification of Candidate Designs

Each candidate design along the random direction is first checked for feasibility at step 4. For aerospace panel design problems the checks for material strength and geometric constraints are relatively quick, and the total time required for checking feasibility is dominated by checks for buckling stability, for each of a number of loading and response cases.

Such a stability check appears to require a full buckling analysis[16] to be performed iteratively to determine the critical buckling load factor. However, a major advantage of the method presented is that it instead uses a single iteration of the Wittrick–Williams algorithm[14] to perform the check. The algorithm normally solves the transcendental buckling eigenproblem by iterating on trial values of the load factor, determining at each iteration the number J of buckling load

factors exceeded by the current trial load factor. Thus the critical buckling load factor is found by converging on the lowest load factor for which $J > 0$. A candidate design is checked for stability by performing a single iteration of the Wittrick–Williams algorithm at the design load: if $J > 0$, the design load exceeds the critical buckling load and the candidate design is infeasible; otherwise, if $J = 0$, the candidate design is feasible.

Figure 1 illustrates that the random direction is able, but unlikely, to traverse the design space with a mass constant at the value for the current best local optimum (f_A). Figure 1 also shows that a feasible candidate design may be in the same valley as the current best local optimum (e.g., C_1) or in a different valley (e.g., C_2). The tunneling check of step 6 determines whether the candidate design is in a different valley by checking whether any part of the straight-line path between the current best local optimum A and the candidate design (C_k, $k = 1, 2, 3$ in Fig. 1) is infeasible, i.e., the random direction has tunneled through a hill into a different valley. To check (approximately) if any part of this straight line is infeasible and to include three common types of hills, i.e., symmetric, skewed to the left, and skewed to the right, three equally spaced points P_k, Q_k, and R_k (which divide the straight line path AC_k into four equal parts) are checked for feasibility. If any of them is infeasible, the candidate design is confirmed to be in a different valley (see step 7) and is used as a starting point for convergence on the new local optimum at the base of this valley. This new local optimum may not be a better local optimum. If all three points at step 6 are feasible, the recovery procedure of step 8 is initiated to further clarify whether the candidate design is indeed in the same valley as the current best local optimum.

C. Recovery Procedure

The recovery procedure of step 8 is designed to cater to situations where the tunneling check wrongly appears to show that a feasible candidate design C_k, which would lead to a better local optimum B, is in the same valley as the current best local optimum A. Such situations occur when the hill sandwiched between A and B is either small or flat, e.g., see Fig. 3. This is a schematic plot similar to Fig. 1 in which the three equally spaced points P_k, Q_k, and R_k on the straight line AC_k are all feasible. To step over this small or flat hill, the recovery procedure linearly factors the candidate design C_k along the straight-line path toward the zero origin of the design space, instead of toward A, until the candidate design has the same mass (f_A) as the current best local optimum A. If this factored candidate design is feasible (e.g., D_k in Fig. 3), it must lie within the valley of a better local optimum than A. On the other hand, if the factored candidate design is infeasible (e.g., E_k or F_k in Fig. 3), three more designs are generated on each side of it by linear interpolation and extrapolation between A and E_k (or F_k). These six designs, denoted by crosses in Fig. 3, are, respectively, 0.7, 0.8, 0.9, 1.1, 1.2, and 1.3 times as far from A as E_k (or F_k). They are checked in turn for feasibility, starting with the design farthest from A. Any of these designs, if feasible, must lie within the valley of the better optimum B.

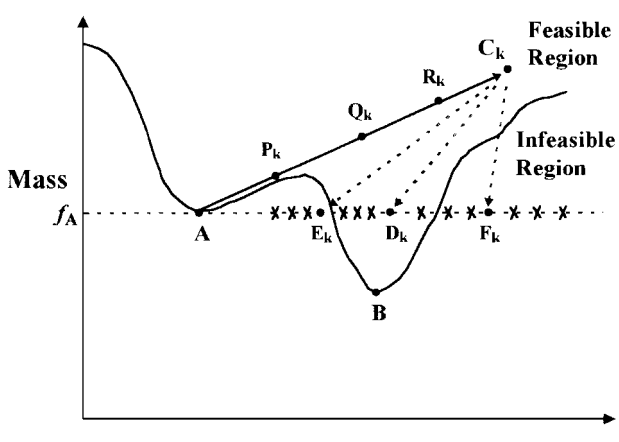

Fig. 3 Illustration of the recovery procedure of step 8 to locate the valley of a better local optimum. The labeled points denoted by • are defined in the text. The unlabeled points denoted by × are linear interpolations and extrapolations used in the recovery procedure.

If no feasible designs are found by the recovery procedure, the candidate design C_k is assumed to be within the valley of the current best local optimum A. Thus the random direction used is abandoned, and the search continues with another random direction.

D. Upper and Lower Tunneling Masses

The tunneling check of step 6 is unable to detect whether a feasible candidate design is in a previously found valley of higher base (i.e., local optimum) mass than that of the current best local optimum (f_A). Therefore, an upper tunneling mass f_T is used, in conjunction with step 2, to prevent tunneling back into a previously found valley. f_T is set to the higher mass of the best two local optima found so far and is updated accordingly whenever a new local optimum is converged on. If the mass of the candidate design most remote from the current best local optimum along the random direction is higher than f_T, then the random direction is abandoned in step 2, and another random direction is generated.

When only one local optimum has been found, f_T is arbitrarily set to some percentage (e.g., 20%) above f_A, to prevent finding valleys that would lead to other but probably not better local optima.

A feasible candidate design having a mass lower than f_A is certain to be in the valley of a better local optimum. Because a valley narrows toward its base, the probability of finding such a feasible candidate design is very small. To save the effort that would have been wasted in showing candidate designs of mass lower than f_A to be infeasible, f_A is regarded as a lower tunneling mass. Thus any random direction whose most remote candidate design from the current best local optimum has a mass lower than f_A is rejected in step 2.

Because of the different weights of contribution of each design variable to the mass, the mass varies only approximately linearly as the design variables are varied linearly between two points within the design space. Therefore the straight lines shown in Figs. 1 and 3 are only approximately straight. Nevertheless, this fact does not affect the main features of the strategy presented. However, during the feasibility check, along a random direction a design may have a mass higher than f_T or lower than f_A, in which case the random direction is abandoned.

E. Termination Criterion

When no additional local optima are found after a certain (large) number of random directions have been searched along (see step 11), the strategy terminates, and the best local optimum converged on is deemed to be the global optimum.

IV. Further Enhancements

A. Design Distinction Criterion

A simple arithmetic mean α is used as a criterion to distinguish two designs: A and G. α is defined as

$$\alpha = \frac{1}{n}\sum_{i=1}^{n}\frac{|x_{Gi} - x_{Ai}|}{x_{ui} - x_{li}} \tag{4}$$

This arithmetic mean α is a numerical measure of how far apart, within the design space, are the best converged local optimum A and the candidate design G. G can be any design along the random direction being searched, one of the designs E_k, D_k, and F_k of Fig. 3, or any interpolated/extrapolated design between A and E_k or F_k. Therefore accepting, as a new starting design, only a suitable feasible design with an α value greater than a user-specified value further ensures a different (better) local optimum is to be converged on. Hence only designs along the random direction, with α greater than some specified value α_{min}, should be checked for feasibility. This requirement is achieved by setting the number of candidate designs, evenly spread along the random direction, equal to the nearest integer below $\alpha_{max}/\alpha_{min}$, where α_{max} is the α value of the candidate design at the furthest point in the random direction from the best converged local optimum. There should also be a maximum number (e.g., 10) of candidate designs to be distributed along the random direction.

B. Restricting the Design Space

When two local optima are converged on, the upper tunneling mass is likely to be very close to the lower tunneling mass, typically only a few percent higher. Therefore it is very demanding to search the entire design space randomly to find a design with a mass between the upper and lower tunneling masses. Therefore, restricting the design space, during the random search only, would be beneficial. The two best converged local optima provide good guidance on how to restrict the design space as other (better) local optima are likely to lie within the proximity of these two distinct local optima. Hence each dimension of the design space is restricted such that, with the best converged local optimum as the center point, the distance between the new lower and upper bounds is a certain percentage (e.g., 200%) of the distance between the two converged local optima. Hence, the new restricted design space encloses the two converged local optima and some space beyond. The new restricted design space remains subject to the user-imposed lower and upper bounds, and so it may be smaller than when simply restricted in the way just described. Restricting the design space has another benefit. If any design variable has the same or very similar values for the two converged local optima, restricting the design space effectively removes the design variable from the problem and hence reduces the number of independent design variables. This in turn reduces the complexity of the problem and hence further improves the efficiency of the random searching process.

V. Numerical Examples

A. Example 1

The first example problem is the minimum-mass stability design of the simply supported metallic aerospace panel shown in Fig. 4, which comprises a skin of thickness t_s stiffened by nine blades with alternating height (h_1, h_2) and thickness (t_1, t_2), equally spaced as shown in Fig. 4a. The five dimensions shown in Fig. 4b were taken as independent design variables. In contrast to previous generalized solutions,[17] the panel was arbitrarily set to be of length $L = 0.32$ m and breadth $B = 0.2$ m. Young's modulus, Poisson's ratio, and the density of the material were, respectively, 65 GPa, 0.3, and 2500 kg/m^3. The panel was longitudinally compressed by a load of 104 kN, and no material strength constraints were imposed. The buckling analysis used half-wavelengths in the range $0.08B$ to L to cover all possible modes of failure. The plate thicknesses were all constrained to lie between 0.45 and 4.05 mm, and the stiffener heights between 5 and 45 mm. Reference 17 showed that the panels of Figs. 4a (variant 1) and 4b (variant 2) are within the valleys of two distinct local optima with the variant 2 optimum being the better of the two.

Table 1 illustrates the hybrid global optimization process. The variant 1 optimum shown in the third column, which is the worse of the two optima, was first converged on using the VICONOPT design procedure, starting from the infeasible initial design specified in the second column of the table. After searching along 22 random directions, the strategy found a feasible candidate design, which is shown in the penultimate column of Table 1. This design is of the variant 2 type and was confirmed, by the tunneling check, to be in a different valley to the variant 1 optimum previously found. The candidate design was then used as a new starting design for the VICONOPT design procedure, which led to convergence on the variant 2 optimum shown in the final column of Table 1, whose mass is 5.6% less than that of the variant 1 optimum. One hundred more random directions were searched along for other suitable starting designs. As no further local optima were found, the variant 2 optimum was deemed to be the global optimum.

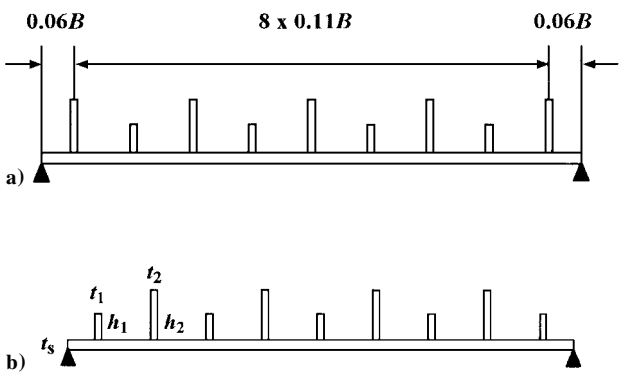

Fig. 4 Two distinct local optima of example 1 showing a) the variant 1 optimum with the stiffener spacing and b) the variant 2 optimum with the five independent design variables.

Table 1 Values of the initial design, variant 1 optimum, feasible candidate design, and the variant 2 optimum of example 1

Design variables	Initial design (infeasible)	Variant 1 optimum (local)	Feasible candidate design	Variant 2 optimum (global)
h_1, mm	24.0	21.6	12.6	9.51
h_2, mm	12.0	9.68	23.5	21.5
t_s, mm	0.60	0.717	0.562	0.695
t_1, mm	1.80	1.91	1.18	0.781
t_2, mm	0.60	0.705	2.54	2.07
Mass, g	292	301	340	284
α	——	0.000	0.266	0.259

The upper tunneling mass was initially set 20% higher than the mass of the first converged variant 1 local optimum, i.e., 361 g. With $\alpha_{\min}$ set to 0.02 and the maximum number of designs along one random direction set to 10, a total of 165 designs along 22 random directions were checked for feasibility, and 17 other designs were abandoned. This represents a 17% saving of searching time compared to that if the number of designs along each random direction is fixed at 10, i.e., a total of 220 designs. The α values of the feasible candidate design and the variant 2 optimum are 0.266 and 0.259, respectively. Both α values are well above the specified minimum of 0.02, indicating that the two local optima are well separated; this is expected as the two local optima have very different physical characteristics. The variant 1 optimum has four short and five tall blade stiffeners whereas the variant 2 optimum has the opposite, five short and four tall blade stiffeners.

A separate run illustrated the necessity of the use of the upper tunneling mass, as follows. Following convergence on the variant 2 optimum, the upper tunneling mass f_T was artificially increased to 40% above the 301 g mass of the variant 1 optimum. The strategy found a feasible candidate design, which, when used as a new starting design, would lead to convergence on the variant 1 optimum. This run showed that, without an appropriate value for the upper tunneling mass, it is possible to tunnel back into a previously found valley.

B. Example 2

The second example problem is one of the problems studied by the Group for Aeronautical Research and Technology in Europe (GARTEUR) Working Group on Structural Optimization.[18] Figure 5 shows the eight panels of the top skin of the Dornier 45-deg swept composite wing. Panel P2, shown in Fig. 6, is a blade stiffened panel with four equally spaced identical blade stiffeners. The panel is assumed to be rectangular and prismatic and carries in-plane longitudinal, transverse, and shear loads. The panel was minimized on mass subject to the constraints of buckling, material strength, and geometric conditions for three load cases. Figure 6 shows the geometry and layup details of the panel. The seven independent design variables were the web height and ply thicknesses for the skin and the web, i.e., h, $t(\pm 45)_s$, $t(0)_s$, $t(90)_s$, $t(\pm 45)_w$, $t(0)_w$, and $t(90)_w$, as shown in Fig. 6. Thirteen point supports were positioned, as illustrated in Fig. 6, to represent simply supported end conditions. The lower and upper bounds for web height were, respectively, 0.5 and 32.5 mm. The ply thicknesses were limited to lie between lower and upper bounds of 0.125 and 5 mm, respectively. The ply properties were $E_{11} = 125$ GPa, $E_{22} = 8.8$ GPa, $G_{12} = G_{13} = 5.3$ GPa, $G_{23} = 0.5\,G_{13} = 2.65$ GPa, $\nu_{12} = 0.35$, and density $= 1620$ kg/m^3. The upper tunneling mass was set initially to 30% above the first converged local optimum, and then it was adjusted in the way described in Sec. III.D when other local optima were converged on. $\alpha_{\min}$ was set to 0.02.

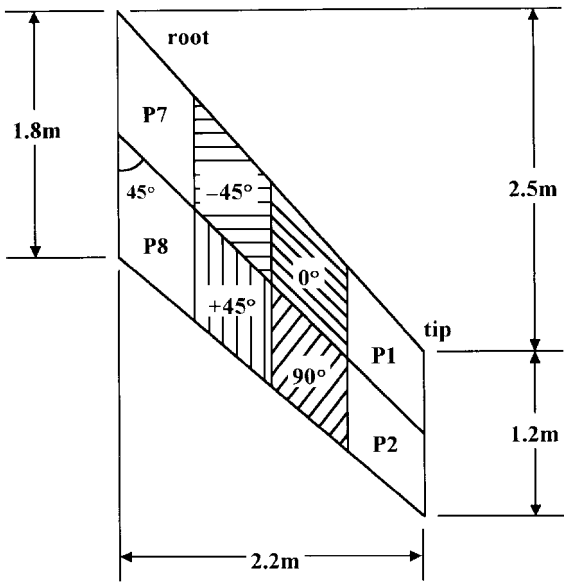

Fig. 5 Plan view of the top skin of the Dornier 45-deg swept composite wing. Four of the eight panels are labeled. Fiber orientations are also indicated.

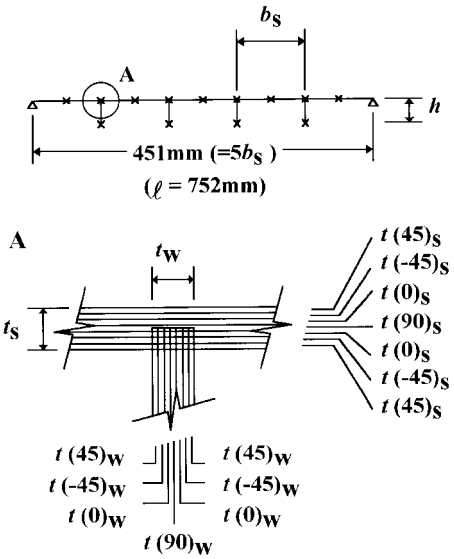

Fig. 6 Cross section of panel P2, showing geometry and layup details. h, $t(\theta)_s$, and $t(\theta)_w$ are the independent design variables. Crosses denote positions of point supports. Ply orientations for skin and webs correspond to the directions illustrated in Fig. 5.

Shown in Table 2 are two local optima, 1 and 2, that are similar in physical characteristics, i.e., optimum 2 is a refinement of optimum 1. They are similar to the two local optima found in the GARTEUR study.[18] Like the first example, the local optimum of higher mass, i.e., optimum 1, was first converged on. As optima 1 and 2 share the same characteristics, the hill sandwiched between them may be very small or flat. This is the type of difficult situation the recovery procedure is designed to resolve. As expected, the recovery procedure did find a feasible candidate design, which, when used as a new starting design, led to convergence on the optimum 2 shown in Table 2. The feasible candidate design, shown in Table 2, was interpolated between points A and F_k of Fig. 3. Because of the similarity of the two converged local optima, optima 1 and 2, the design space was restricted during the random search to designs with the characteristics of these optima, and no additional local optimum was found.

The VICONOPT design procedure first defines a small subdesign space around the starting design within which it, guided by the feasible directions, searches for better feasible designs. This subdesign space around the current best feasible design diminishes as the design procedure progresses until convergence. Restarting the VICONOPT design procedure resets the subdesign space to its default size, and using the converged final design as the new starting design may step over the small or flat hill. Table 3 shows that, using optimum 1 as the new starting design, an optimum close to optimum 2 was converged on. At this point, because only one local optimum, i.e., optimum 2, has been found, the design space remained at its initially user-specified size. This enabled a suitable starting design of different characteristics to be found by the searching process of the hybrid global optimization strategy.

Table 2 Values of the initial design, optimum 1, feasible candidate design, and optimum 2 of example 2

Design variables	Initial design (infeasible)	Optimum 1 (local)	Feasible candidate design	Optimum 2 (global)
h, mm	16.25	32.50	32.2	32.5
$t(\pm 45)_s$, mm	0.125	0.584	0.547	0.525
$t(0)_s$, mm	0.125	0.735	0.501	0.582
$t(90)_s$, mm	0.125	0.125	0.125	0.136
t_s, mm	0.875	3.93	3.31	3.40
$t(\pm 45)_w$, mm	0.125	0.125	0.125	0.136
$t(0)_w$, mm	0.125	2.25	3.36	3.08
$t(90)_w$, mm	0.125	0.125	0.125	0.125
t_w, mm	0.875	5.13	7.35	6.84
Mass, g	550	2974	2975	2950
α	——	0.000	0.042	0.031

The second starting design, shown in Table 3, differs significantly from optima 1 and 2 in that, for the skin, the 0-deg ply $t(0)_s$ is much thinner, and the 90-deg ply $t(90)_s$ is substantially thicker. This design was, as expected, confirmed to be in a different valley by the tunneling check. The better optimum 3, shown in Table 3, was converged on from this second starting design. The two optima found so far, i.e., optima 2 and 3, despite their differences, shared some common characteristics. Their values of h, $t(\pm 45)_w$, and $t(90)_w$ were almost identical. Hence, after the design space was appropriately restricted to enclose the two optima, the variables h, $t(\pm 45)_w$, and $t(90)_w$ were effectively removed from the problem. The number of independent design variables was thus reduced from seven to four.

The hybrid global optimization strategy continued to search in the newly restricted design space and found a feasible candidate design that was shown to be unsuitable as a new starting design by the tunneling check. This design was thus factored, i.e., to D_k of Fig. 3, and confirmed to be suitable by the recovery procedure for use as the third starting design, shown in Table 3, which is fairly similar to optimum 3. Optimum 4 of Table 3 was converged on from this third starting design. Table 3 shows that optimum 4 is a refinement of optimum 3 with a 1.0% mass reduction. No additional local optimum was found after 100 further random directions were searched. The best local optimum converged on, i.e., optimum 4, was deemed to be the global optimum.

Two attempts were also made to use optima 2 and 3, separately, as the initial starting design for the VICONOPT design procedure to converge onto a better local optimum. Both attempts failed to converge onto the better local optimum, i.e., from optimum 2 to optimum 3 and from optimum 3 to optimum 4. In this context the need for the hybrid global optimization strategy, particularly the random search and the recovery procedure, is justified. Optima 3 and 4 offer further mass savings of 1.1 and 2.1%, respectively, compared to the best optimum, i.e., optimum 2, found in the GARTEUR study.[18] Although such mass savings are quite small, they would produce significant savings in manufacturing and operating costs if replicated over an entire aircraft wing.

In this study it was not possible to compare directly the computational effort required by the proposed method with that required by competing methods. However, the inclusion of directed search techniques for convergence on local optima greatly reduces the number of function evaluations compared with purely random search methods. Moreover, the methods used to solve the transcendental buckling eigenproblem enable many of the iterative constraint calculations that dominate VICONOPT's purely directed search to be replaced here by single iteration feasibility checks.

Table 3 Progress of the global optimization process of example 2, showing the details of the starting designs and the converged optima

Design variables	Initial starting design (optimum 1)	First converged optimum (~ optimum 2)	Second starting design	Second converged optimum (optimum 3)	Third starting design	Converged global optimum (optimum 4)
h, mm	32.5	32.5	27.3	32.5	32.2	32.5
$t(\pm 45)_s$, mm	0.584	0.517	0.441	0.392	0.238	0.226
$t(0)_s$, mm	0.735	0.566	0.471	0.125	0.125	0.125
$t(90)_s$, mm	0.125	0.125	1.77	2.14	2.49	2.55
t_s, mm	3.93	3.32	4.48	3.96	3.70	3.71
$t(\pm 45)_w$, mm	0.125	0.125	0.125	0.125	0.125	0.125
$t(0)_w$, mm	2.25	3.23	2.97	2.04	2.51	2.38
$t(90)_w$, mm	0.125	0.125	0.125	0.125	0.125	0.125
t_w, mm	5.13	7.09	6.57	4.70	5.64	5.38
Mass, g	2974	2950	3334	2918	2917	2888
α	——	0.000	0.084	0.111	0.113	0.118
——	——	——	——	(0.000)[a]	(0.088)	(0.089)

[a]The values in parentheses are the α values when optimum 3 is the datum and the design space is restricted.

VI. Conclusions

A hybrid global optimization strategy has been presented. The strategy combines the tunneling and IHR optimization methods with a directed search method. The strategy has unique features because of the underlying structural theory being exact, in the sense of differential equations being solved for the member (or element) stiffnesses so that they are transcendental functions of the load factor. Hence, the buckling eigenproblem for the entire structure is a transcendental one, instead of the linear one associated with the more usual finite element method formulations. Minimum-mass aerospace panel stability design problems were used as examples to demonstrate the efficiency and robustness of the global optimization strategy and to illustrate the following features of the strategy presented.

The global optimum is found by successively converging on better local optima. Each converged local optimum is escaped from by using a biased random search to find a suitable starting design, which, as shown by the tunneling check, will lead to a different, possibly better, local optimum. The random search is further assisted, by the recovery procedure, to find suitable starting designs in a valley that is separated from the best converged local optimum by a small or flat hill. The use of an upper tunneling mass prevents the possibility of returning to previously found local optima.

The hybrid global optimization strategy is mainly based on the directed search feasible directions optimization method. Some features of the strategy can be shown to be analogous to other optimization methods. For example, the reduction in the number of independent design variables, via the design space restriction, is similar to the selection of parents in genetic algorithms. The concept of the hybrid strategy presented is to combine the advantageous features of different optimization methods into a more efficient and robust global optimization strategy, as illustrated in this paper.

Acknowledgments

The authors gratefully acknowledge financial support from the Engineering and Physical Sciences Research Council under Grant GR/J79430. Useful discussions with P. W. L. Williams and C. B. York are also acknowledged.

References

[1]Rozvany, G. I. N., *Structural Design via Optimality Criteria: The Prager Approach to Structural Optimization*, 1st ed., Kluwer, Dordrecht, The Netherlands, 1989, pp. 1–20.

[2]Vanderplaats, G. N., and Moses, F., "Structural Optimization by Methods of Feasible Directions," *Computers and Structures*, Vol. 3, No. 4, 1973, pp. 739–755.

[3]Hajela, P., "Genetic Search—An Approach to the Nonconvex Optimization Problem," *AIAA Journal*, Vol. 28, No. 7, 1990, pp. 1205–1210.

[4]Le Riche, R., and Haftka, R. T., "Optimization of Laminate Stacking Sequence for Buckling Load Maximization by Genetic Algorithm," *AIAA Journal*, Vol. 31, No. 5, 1993, pp. 951–956.

[5]Lin, C.-Y., and Hajela, P., "Design Optimization with Advanced Genetic Search Strategies," *Advances in Engineering Software*, Vol. 21, No. 3, 1994, pp. 179–189.

[6]Nagendra, S., Jestin, D., Gürdal, Z., Haftka, R. T., and Watson, L. T., "Improved Genetic Algorithm for the Design of Stiffened Composite Panels," *Computers and Structures*, Vol. 58, No. 3, 1996, pp. 543–555.

[7]Atiqullah, M. M., and Rao, S. S., "Parallel Processing in Optimal Structural Design Using Simulated Annealing," *AIAA Journal*, Vol. 33, No. 12, 1995, pp. 2386–2392.

[8]Levy, A. V., and Gomez, S., "The Tunneling Method Applied to Global Optimization," *Numerical Optimization 1984*, edited by P. T. Boggs, R. H. Byrd, and R. B. Schnabel, Society for Industrial and Applied Mathematics, Philadelphia, PA, 1985, pp. 213–244.

[9]Zabinsky, Z. B., Smith, R. L., McDonald, J. F., Romeijn, H. E., and Kaufman, D. E., "Improving Hit-and-Run for Global Optimization," *Journal of Global Optimization*, Vol. 3, No. 2, 1993, pp. 171–192.

[10]Zabinsky, Z. B., "Global Optimization for Composite Structural Design," *Proceedings of the AIAA/ASME/ASCE/AHS/ASC 35th Structures, Structural Dynamics, and Materials Conference*, Vol. 3, AIAA, Washington, DC, 1994, pp. 1406–1412.

[11]Snyman, J. A., and Stander, N., "New Successive Approximation Method for Optimum Structural Design," *AIAA Journal*, Vol. 32, No. 6, 1994, pp. 1310–1315.

[12]Butler, R., and Williams, F. W., "Optimum Design Using VICONOPT, a Buckling and Strength Constraint Program for Prismatic Assemblies of Anisotropic Plates," *Computers and Structures*, Vol. 43, No. 4, 1992, pp. 699–708.

[13]Edwards, D. A., Williams, F. W., and Kennedy, D., "Cost Optimization of Stiffened Panels Using VICONOPT," *AIAA Journal*, Vol. 36, No. 2, 1998, pp. 267–272.

[14]Wittrick, W. H., and Williams, F. W., "An Algorithm for Computing Critical Buckling Loads of Elastic Structures," *Journal of Structural Mechanics*, Vol. 1, No. 4, 1973, pp. 497–518.

[15]Press, W. H., Flannery, B. P., Teukolsky, S. A., and Vetterling, W. T., *Numerical Recipes: The Art of Scientific Computing*, 1st ed., Cambridge Univ. Press, Cambridge, England, UK, 1986, pp. 191–225.

[16]Wittrick, W. H., and Williams, F. W., "Buckling and Vibration of Anisotropic or Isotropic Plate Assemblies Under Combined Loadings," *International Journal of Mechanical Sciences*, Vol. 16, No. 4, 1974, pp. 209–239.

[17]Butler, R., and Williams, F. W., "Optimum Buckling Design of Compression Panels Using VICONOPT," *Structural Optimization*, Vol. 6, No. 3, 1993, pp. 160–165.

[18]York, C. B., Williams, F. W., Kennedy, D., and Butler, R., "A Parametric Study of Optimum Designs for Benchmark Stiffened Wing Panels," *Composites Engineering*, Vol. 3, Nos. 7, 8, 1993, pp. 619–632.

A. Chattopadhyay
Associate Editor